Applications in Engineering Science 14 (2023) 100126

Contents lists available at ScienceDirect

Applications in Engineering Science

journal homepage: www.elsevier.com/locate/apples

Mechanical response of elastic materials with density dependent Young modulus☆

Vít Průša *, Ladislav Trnka

Faculty of Mathematics and Physics, Charles University, Sokolovská 83, Praha 8 – Karlín, CZ 186 75, Czech Republic

ARTICLE INFO

MSC:
74B05

Keywords:
Elasticity
Infinitesimal deformations
Density dependent material moduli

ABSTRACT

The experimental as well as theoretical engineering literature on porous structures such as metal foams, aerogels or bones often relies on the standard linearised elasticity theory, and, simultaneously, it frequently introduces the concept of "density dependent Young modulus". We interpret the concept of "density dependent Young modulus" literally, that is we consider the linearised elasticity theory with the generalised Young modulus being a function of the current density, and we briefly summarise the existing literature on theoretical justification of such models. Subsequently we numerically study the response of elastic materials with the "density dependent Young modulus" in several complex geometrical settings.

In particular, we study the extension of a right circular cylinder, the deflection of a thin plate, the bending of a beam, and the compression of a cube subject to a surface load, and we quantify the impact of the density dependent Young modulus on the mechanical response in the given setting. In some geometrical settings the impact is almost nonexisting—the results based on the classical theory with the constant Young modulus are nearly identical to the results obtained for the density dependent Young modulus. However, in some cases such as the deflection of a thin plate, the results obtained with constant/density dependent Young modulus differ considerably despite the fact that in both cases the infinitesimal strain condition is well satisfied.

1. Introduction

The engineering literature on porous structures such as metal foams, Gibson (2000), Gibson and Ashby (1982), Roberts and Garboczi (2001), aerogels, Chandrasekaran et al. (2017), Leventis et al. (2002) or bones, Rice et al. (1988), often introduces the concept of "density dependent Young modulus". For example, the Young modulus E is being considered in the power-law form

$$\mathrm{E}(\rho) = \mathrm{E}_{\mathrm{ref}} \left(\frac{\rho}{\rho_{\mathrm{R}}} \right)^{n}, \tag{1}$$

where ρ denotes the current material density, ρ_{R} denotes the reference material density, $\mathrm{E}_{\mathrm{ref}}$ denotes the Young modulus at the reference density, and n is a given exponent. The very notion of Young modulus is however intimately related to the *standard* linearised elasticity, and the concept of density dependent Young modulus leads to contradictory statements.

On the one hand the basic premise of the standard linearised elasticity theory is that the stress tensor can be expressed as a linear function of the infinitesimal (linearised) strain tensor, wherein the Young modulus plays the role of a constant coefficient. On the other hand the Young modulus in the given linear constitutive relation is subsequently assumed to be a density-dependent quantity. But the density-dependence of Young modulus implies—in virtue of the balance of mass—the dependence of Young modulus on the linearised strain tensor, which in turn leads to a nonlinear stress–strain relation. This contradicts the initial assumption on linearity of the constitutive relation.

The contradiction can be remedied using the concept of implicit constitutive relations, that allows one to transparently justify nonlinear constitutive relations in the infinitesimal strain regime, see Rajagopal and Saccomandi (2022) for a recent discussion thereof. (For further discussion see also Rajagopal, 2014, 2018, 2021.) Despite the sound theoretical justification of infinitesimal strain models with the density dependent Young modulus, and their prospective importance in the study of mechanical response of various materials, only *few works have been so far devoted to the quantification of effects due to the density dependent Young modulus*, see Murru and Rajagopal (2021b,a), Vajipeyajula et al. (2022) or Průša et al. (2022) for examples thereof. In our current contribution we aim at such quantification. In particular, we *numerically study* the response of elastic materials with density dependent

☆ Vít Průša thanks the Czech Science Foundation, grant number 20-11027X, for its support.
* Corresponding author.
E-mail addresses: prusv@karlin.mff.cuni.cz (V. Průša), ladtrnjr@volny.cz (L. Trnka).

https://doi.org/10.1016/j.apples.2023.100126
Received 29 November 2022; Received in revised form 30 January 2023; Accepted 1 February 2023
Available online 7 February 2023

Young modulus in several geometrical settings—the extension of a right circular cylinder, the deflection of a thin plate, the bending of a beam, and the compression of a cube subject to a surface load.

2. Infinitesimal strain models for elastic bodies with density dependent Young modulus

In the framework of the standard linearised elasticity the concept of Young modulus is well defined. The standard linear constitutive relation for isotropic elastic materials takes the form

$$\mathfrak{e} = \frac{1}{\mathrm{E}}\left[(1+\nu)\mathfrak{t} - \nu(\mathrm{Tr}\,\mathfrak{t})\mathbb{I}\right], \tag{2}$$

where the Young modulus E and the Poisson ratio ν are constant material parameters, and the symbols $\mathfrak{e}$ and $\mathfrak{t}$ denote the infinitesimal strain tensor and the stress tensor respectively. The standard linearised constitutive relation (2) that holds for isotropic elastic materials in the small strain regime is however also used with "density dependent Young modulus", wherein the Young modulus is given, for example, by the power-law formula (1). The density dependent Young modulus in the form (1) can be interpreted in two different ways.

First, the concept of "density dependent Young modulus" can serve as a very simple description of the material inner structure (porous structure). In this case, the relative material density is a simple tool for characterisation of number/volume of voids in the material of interest, and the Young modulus is a *constant for the given material structure*. It is not interpreted as a function of the *current density* of the material—even if the current density of the material might change due to the deformation of the material.

Second, the concept of "density dependent Young modulus" can be taken literally. In this case the Young modulus is interpreted as a function of the *current density*, and its value must be updated whenever the material undergoes a deformation. Consequently, it would be more appropriate to talk about a *generalised Young modulus*, since we are replacing a constant material parameter by a material function. (In principle, the situation is the same as in theory of non-Newtonian fluids, wherein one introduces the apparent/effective viscosity instead of constant viscosity for the standard Navier–Stokes fluid.) In our current contribution we follow this interpretation of "density dependent (generalised) Young modulus". The constitutive relation can be then obtained by the simple substitution of formula of type (1) into (2),

$$\mathfrak{e} = \frac{1}{\mathrm{E}(\rho)}\left[(1+\nu_{\mathrm{ref}})\mathfrak{t} - \nu_{\mathrm{ref}}(\mathrm{Tr}\,\mathfrak{t})\mathbb{I}\right], \tag{3}$$

where the *reference* Young modulus $\mathrm{E}_{\mathrm{ref}}$ and the *reference* Poisson ratio ν_{ref} are related to the reference configuration, and they are constant material parameters. As we have already noted, this *ad hoc* model is however not consistent with the basic principles of standard linearised elasticity that admits only *linear* relation between the stress and infinitesimal strain tensors. But models of this type can be justified by a linearisation (infinitesimal strain) of implicit constitutive relation in the nonlinear elasticity theory, see Rajagopal and Saccomandi (2022) and also remarks in Průša et al. (2020).

In general, the density equation reads $\rho_{\mathrm{R}} = \rho \det \mathbb{F}$, where $\mathbb{F}$ denotes the deformation gradient. Under the infinitesimal strain assumption, the density equation is approximated by $\rho_{\mathrm{R}} \approx \rho(1+\mathrm{Tr}\,\mathfrak{e})$, and upon linearisation of (1) with respect to $\mathfrak{e}$ we obtain

$$\mathrm{E}(\rho) \approx \mathrm{E}_{\mathrm{ref}}\,(1 - n\,\mathrm{Tr}\,\mathfrak{e})\,. \tag{4}$$

Consequently, the *ad hoc* constitutive relation takes the form

$$\mathfrak{e} = \frac{1+\nu_{\mathrm{ref}}}{\mathrm{E}_{\mathrm{ref}}\,(1-n\,\mathrm{Tr}\,\mathfrak{e})}\mathfrak{t} - \frac{\nu_{\mathrm{ref}}}{\mathrm{E}_{\mathrm{ref}}\,(1-n\,\mathrm{Tr}\,\mathfrak{e})}(\mathrm{Tr}\,\mathfrak{t})\mathbb{I}, \tag{5}$$

which under the infinitesimal strain assumption and in virtue of approximation $\frac{1}{1-x} \approx 1+x$ further reduces to

$$\mathfrak{e} = \frac{1}{\mathrm{E}_{\mathrm{ref}}}\,(1+n\,\mathrm{Tr}\,\mathfrak{e})\left[(1+\nu_{\mathrm{ref}})\mathfrak{t} - \nu_{\mathrm{ref}}(\mathrm{Tr}\,\mathfrak{t})\mathbb{I}\right]. \tag{6}$$

We see that the basic assumption of implicit type constitutive theory for nonlinear elastic bodies is essential in this manipulation. Unlike the standard nonlinear elasticity theory that starts with the assumption $\mathbb{T} = \mathfrak{f}(\mathbb{B})$, the implicit theory starts with the constitutive relation in the form $\mathfrak{f}(\mathbb{T},\mathbb{B}) = \mathbb{O}$. (See Rajagopal (2003), Muliana et al. (2018) and Bustamante and Rajagopal (2020, 2021) for a discussion of this seemingly minor change in the fundamental constitutive assumption, and its impact on the modelling of nonlinear elastic response of solids.) In the former case of the standard nonlinear elasticity theory the linearisation $\mathbb{B} \approx 1 + 2\mathfrak{e}$ can only lead to a linear constitutive relation $\mathfrak{t} = \mathfrak{g}(\mathfrak{e})$, where $\mathfrak{g}$ is a linear function. The implicit relation $\mathfrak{f}(\mathbb{T},\mathbb{B}) = \mathbb{O}$ however linearises to $\mathfrak{g}(\mathfrak{t},\mathfrak{e}) = \mathbb{O}$, where $\mathfrak{g}$ is a *bilinear function* of $\mathfrak{e}$ and $\mathfrak{t}$—an example thereof is (6), see Rajagopal (2018) for further discussion. If needed the constitutive relation (6) can be manipulated into the form

$$\mathfrak{t} = \alpha_{\mathrm{ref}}(1 - n\,\mathrm{Tr}\,\mathfrak{e})\,(\mathrm{Tr}\,\mathfrak{e})\,\mathbb{I} + 2\beta_{\mathrm{ref}}(1 - n\,\mathrm{Tr}\,\mathfrak{e})\mathfrak{e}, \tag{7}$$

where we denote

$$\alpha_{\mathrm{ref}} =_{\mathrm{def}} \frac{\nu_{\mathrm{ref}}\mathrm{E}_{\mathrm{ref}}}{(1+\nu_{\mathrm{ref}})(1-2\nu_{\mathrm{ref}})}, \qquad \beta_{\mathrm{ref}} =_{\mathrm{def}} \frac{\mathrm{E}_{\mathrm{ref}}}{2(1+\nu_{\mathrm{ref}})}. \tag{8}$$

Note that this form requires one to do another linearisation with respect to $\mathfrak{e}$, see again Rajagopal (2018) for a detailed discussion of subtleties of linearisation of constitutive relations in nonlinear elasticity theory, especially in the context of implicit constitutive relations. Clearly, if $n = 0$, then the formula (7) for the stress tensor $\mathfrak{t}$ reduces to the standard form used in the standard linearised elasticity theory

$$\mathfrak{t} = \lambda\,(\mathrm{Tr}\,\mathfrak{e})\,\mathbb{I} + 2\mu\mathfrak{e}, \tag{9}$$

where λ and μ are the standard Lamé parameters.

In what follows we investigate the quantitative behaviour of the model (3) in the infinitesimal strain regime, that is we work with (6), and we compare the predictions based on (6) with the predictions based on the standard linearised elasticity model (9). In particular, using the finite element method we implement numerical solvers for both models, we solve several static boundary value problems, and we compare the predictions obtained by the models. The objective is to quantify the impact of the parameter n to the predicted deformation. (Recall that the value $n = 0$ corresponds to the standard linearised elasticity.) In this regard we recall that the values of n known in the literature are in the order of units, see Průša et al. (2022). The specific problems of interest are the extension of a right circular cylinder, see Section 3.1, the deflection of a thin plate, see Section 3.2, the compression of a cube, see Section 3.3 and the bending of a rectangular prismatic beam, see Section 3.4.

To use the finite element method we reformulate boundary value problems in the weak (variational) form. The static boundary value problem in domain Ω with the boundary $\partial\Omega = \Gamma_D \cup \Gamma_N$ reads

$$\mathrm{div}\,\mathfrak{t}(\boldsymbol{u}) + \boldsymbol{f} = \boldsymbol{0}, \qquad \text{in } \Omega, \tag{10a}$$

$$\boldsymbol{u}|_{\Gamma_D} = \boldsymbol{u}_D, \qquad \text{on } \Gamma_D, \tag{10b}$$

$$\mathfrak{t}\boldsymbol{n}|_{\Gamma_N} = \boldsymbol{g}, \qquad \text{on } \Gamma_N, \tag{10c}$$

where $\boldsymbol{u}$ denotes the displacement field, $\boldsymbol{f}$ denotes the given body force, $\boldsymbol{u}_D$ denotes the given displacement boundary condition, and $\boldsymbol{g}$ denotes the given traction. The weak formulation (10) is then obtained by that standard manipulation. We multiply (10a) by a test function $\boldsymbol{v} \in \hat{V}$ satisfying the Dirichlet boundary conditions on Γ_D, we integrate over the domain Ω, and then we integrate by parts. The weak formulation then requires one to find the displacement field $\boldsymbol{u}$ such that the equation

$$\int_\Omega \mathfrak{t}(\boldsymbol{u}) : \mathfrak{e}(\boldsymbol{v})\,\mathrm{d}x - \int_\Omega \boldsymbol{f}\bullet\boldsymbol{v}\,\mathrm{d}x - \int_{\Gamma_N} \boldsymbol{g}\bullet\boldsymbol{v}\,\mathrm{d}s = 0, \tag{11}$$

holds for all $\boldsymbol{v} \in \hat{V}$, wherein we use the notation $\mathbb{A} : \mathbb{B} =_{\mathrm{def}} \mathrm{Tr}\left(\mathbb{A}\mathbb{B}^{\mathsf{T}}\right)$ for the dot product on the space of matrices, and the notation $\mathfrak{e}(\boldsymbol{v}) =_{\mathrm{def}}$

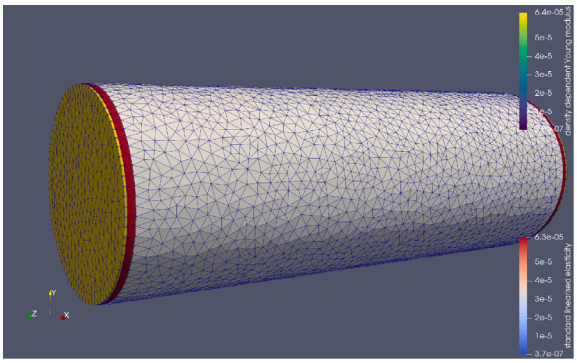

(A) Extension of a right circular cylinder, $n = n_{\max}$; red – prediction by the standard linearised elasticity model, yellow – prediction by the model with density dependent Young modulus.

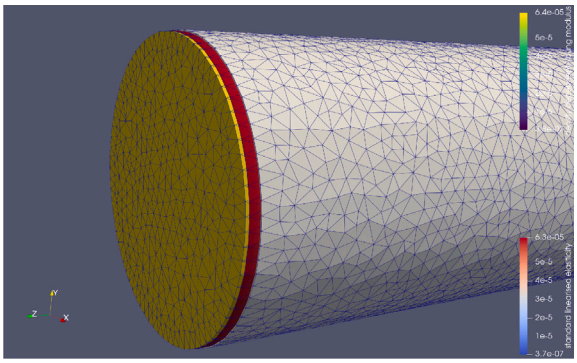

(B) Detailed view on the base of the cylinder, $n = n_{\max}$; red – prediction by the standard linearised elasticity model, yellow – prediction by the model with density dependent Young modulus.

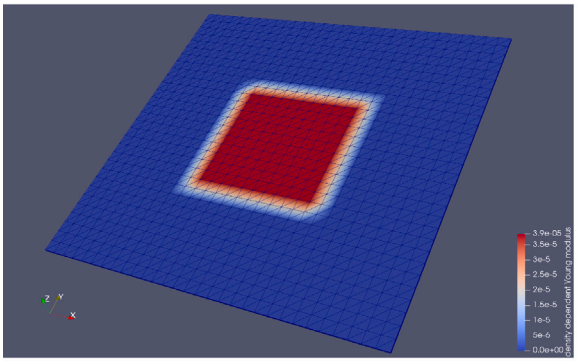

(C) Deflection of a thin plate. The square in the centre is loaded; prediction based on the nonlinear model with $n = n_{\min}$.

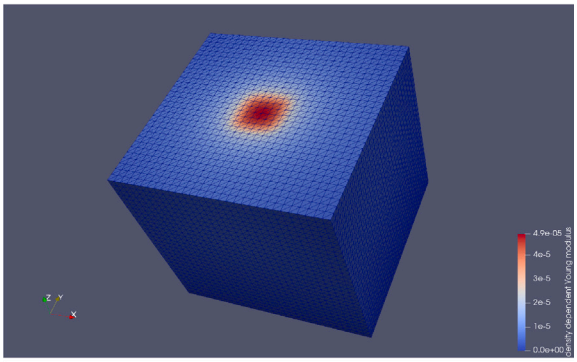

(D) Compression of a cube. The square in the centre is loaded; prediction based on the nonlinear model with $n = n_{\min}$.

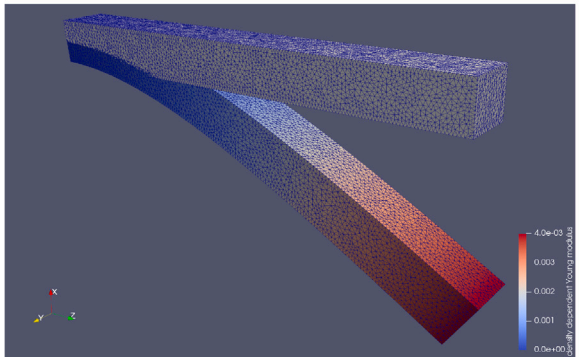

(E) Bending of a beam by the end load; prediction based on the nonlinear model with $n = n_{\max}$.

Fig. 1. Boundary value problems. (For interpretation of the references to colour in this figure legend, the reader is referred to the web version of this article.)

$\frac{1}{2}\left(\nabla \boldsymbol{v} + (\nabla \boldsymbol{v})^{\mathsf{T}}\right)$ and similarly for $\mathbb{T}$. (This notation allows us to distinguish whether we are dealing with the symmetric gradient/linearised strain tensor associated to $\boldsymbol{v}$ or $\boldsymbol{u}$.) Note that in the weak formulation of the governing Eqs. (11) we use the formula (7) for the stress tensor, which effectively gives us the stress $\mathbb{T}$ as a nonlinear function of the linearised strain tensor $\mathbb{C}$.

The numerical solver based on the finite element method is implemented using the FEniCS computing platform, see Logg et al. (2012), Alnæs et al. (2015). For the spatial discretisation of the weak formulation (11), we use the finite dimensional space based on the second order Lagrange element (CG2) for the displacement. The computational meshes are shown in Fig. 1, the dimension of discrete finite element spaces is shown in Table 1. The nonlinear problem (11) is solved directly in FEniCS by its default nonlinear solver based on the Newton method.

3. Solution of boundary value problems

We consider elastic solids whose mechanical response is specified either by the linear constitutive relation (2) or by the nonlinear constitutive relation (7) with a chosen power-law exponent n. In both cases we use the infinitesimal strain approximation with all its benefits such as the straightforward specification of the boundary conditions in the reference configuration and so forth. In all numerical computations we monitor the maximum value (over the nodal points of the computational mesh) of the norm of the linearised strain tensor $\|\mathbb{C}\|_{\infty} =_{\text{def}} \max_{\boldsymbol{x}\in\Omega_h} |\mathbb{C}(\boldsymbol{u}(\boldsymbol{x}))|$, see Table 1. (The linearised strain $\mathbb{C}$ is obtained from the computed displacement field $\boldsymbol{u}$ via the projection to discontinuous Lagrange elements DG0.) Later this allows us to evaluate the validity of the infinitesimal strain approximation.

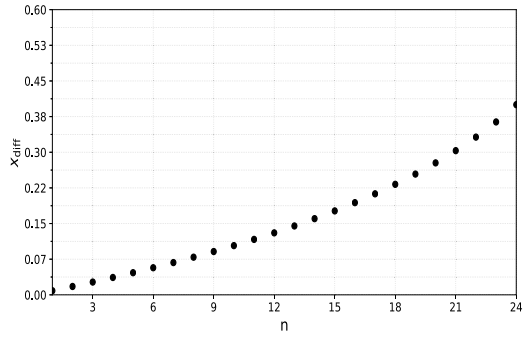

(A) Relative difference between the model predictions x_{diff} as a function of the power-law exponent n; constant applied load.

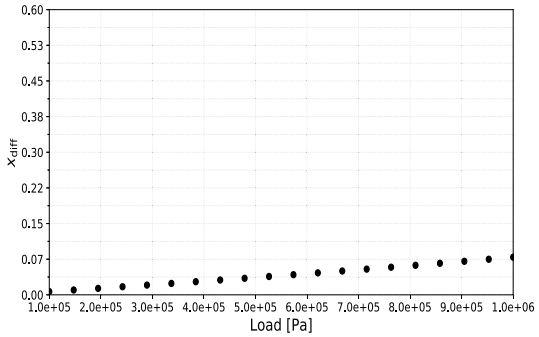

(B) Relative difference between the model predictions x_{diff} as a function of the applied load; constant power-law exponent $n = 4$.

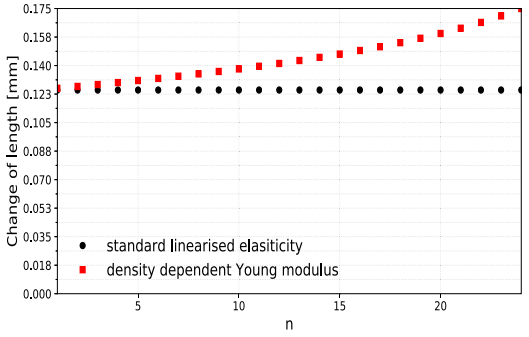

(C) Change of the cylinder length Δl as a function of the power-law exponent n; constant applied load.

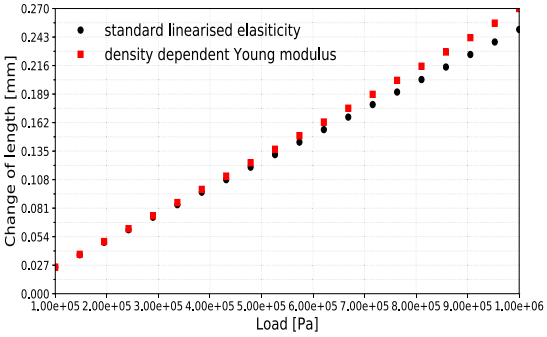

(D) Change of the cylinder length Δl as a function of the applied load; constant power-law exponent $n = 4$.

Fig. 2. Extension of the right circular cylinder, parameters given by Table 1.

In what follows we use subscripts $(\cdot)_{\mathrm{non}}$ and $(\cdot)_{\mathrm{lin}}$ to distinguish between the predictions based on the models with the density dependent Young modulus and the standard linearised elasticity. For each boundary value problem we choose a representative scalar quantity x that characterises the deformation. This quantity can be the elongation of the cylinder, the deflection of the centre of the plate and so forth, see below for detailed specification. Using the quantity x we then compute the relative difference between the prediction based on the model with the density dependent generalised Young modulus and the standard linearised elasticity model,

$$x_{\mathrm{diff}} =_{\mathrm{def}} \left| \frac{x_{\mathrm{lin}} - x_{\mathrm{non}}}{x_{\mathrm{lin}}} \right| .$$

This quantity allows us to quantify the difference between the model predictions by the means of a single representative scalar quantity. Furthermore, in all subsequent plots of x_{diff} versus the power-law exponent n and plots of x_{diff} versus the load we use the same scale on the vertical axis. The objective is again to allow one to quickly assess the impact of "density dependent Young modulus" in various settings.

The specific boundary value problems considered in the present work are the extension of a right circular cylinder, deflection of a thin plate, the compression of a cube and the bending of a beam by an end load. For each problem we compute the solution for various integer values of the power-law exponent n, $n \in \{n_{\min}, \dots, n_{\max}\}$, see Table 1. The value $n_{\max}$ is typically chosen as the maximum value of n for which our straightforward implementation of the Newton method in our finite element method converged to a solution. For fixed $n = 4$ we also compute the solution for various loads/external pressures from a given interval, see Table 1.

3.1. Extension of a right circular cylinder

We consider a right circular cylinder with the radius R and the height l, see Fig. 1(a). On both bases we apply a uniformly distributed constant force $\boldsymbol{F}$ that acts in the direction perpendicular to the base and that is pointing out of the cylinder. (The magnitude of the force $\boldsymbol{F}$ divided by the base area is reported in Table 1 as the load.) The lateral surface is traction free. The values of all relevant parameters are summarised in Table 1.

The pair of forces $\boldsymbol{F}$ stretches the cylinder to the new length $l + \Delta l$. The computed quantity x_{diff} is the relative difference in the extension of the cylinder, that is the relative difference between Δl_{lin} predicted by the linear model (2) and Δl_{non} predicted by the nonlinear model (7). Numerical results are shown in Fig. 2.

3.2. Deflection of a thin plate

We consider a block with spatial dimensions a, b and c whose top base is loaded, see Fig. 1(c). The block thickness c is substantially smaller than the remaining block dimensions, hence we refer to this geometry as the plate geometry. An external load is acting on the top base, and it is uniformly distributed in the square with the side length $\frac{2}{5}a$ that is located at the centre of the top base. The bottom base of the plate is fixed—we prescribe the zero displacement here—and all lateral faces are traction free. The values of all relevant parameters are summarised in Table 1.

The computed quantity x_{diff} is the relative difference between the deflection of the centre of top plate surface as predicted by the linear model (2) and by the nonlinear model (7). In other words the

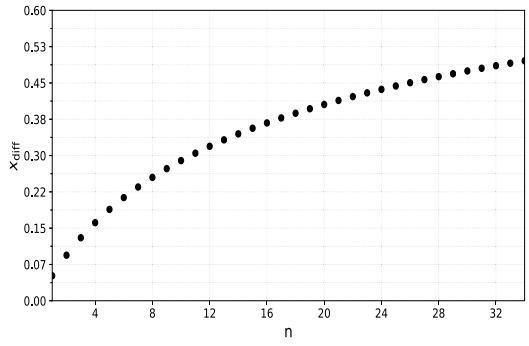

(A) Relative difference between the model predictions x_{diff} as a function of the power-law exponent n; constant applied load.

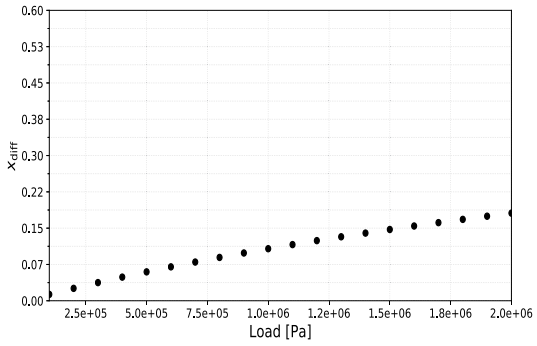

(B) Relative difference between the model predictions x_{diff} as a function of the applied load; constant power-law exponent $n = 4$.

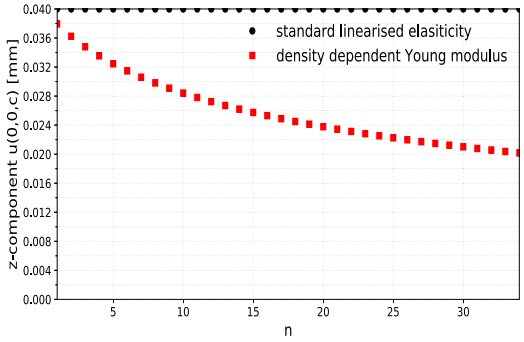

(C) Vertical displacement $\mathrm{u}^z(0,0,0)$ of the top surface centre as a function of the power-law exponent n; constant applied load.

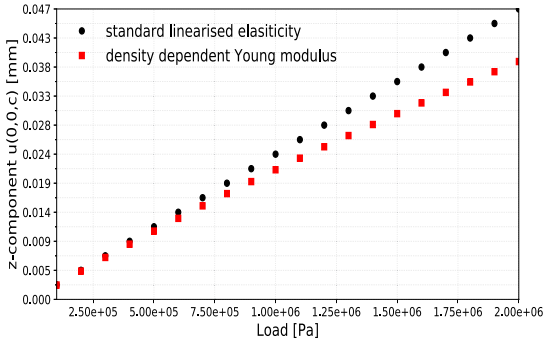

(D) Vertical displacement $\mathrm{u}^z(0,0,0)$ of the top surface centre as as a function of the applied load; constant power-law exponent $n = 4$.

Fig. 3. Deflection of a thin plate, parameters given by Table 1.

Table 1
Parameter values for computations reported in Section 3. Cylinder with radius R and length l; cube, plate and beam with spatial dimensions a, b and c and length l respectively, dimension of finite element function space, generalised Young modulus at reference configuration $\mathrm{E}_{\mathrm{ref}}$, Poisson ratio at reference configuration ν_{ref}, power-law exponent n in the formula for the generalised Young modulus (1), load applied on objects. Computed maximal value of the linearised strain tensor at nodal points of computational mesh, $\|\mathfrak{e}_{\mathrm{lin}}\|_\infty$ and $\|\mathfrak{e}_{\mathrm{non}}\|_\infty$.

Problem	Geometry [mm]	Degrees of freedom	$\mathrm{E}_{\mathrm{ref}}$ [Pa]	ν_{ref}	n_{min}	n_{max}	$\mathrm{Load}_{\mathrm{min}}$ [Pa]	$\mathrm{Load}_{\mathrm{max}}$ [Pa]	$\|\mathfrak{e}_{\mathrm{lin}}\|_\infty$	$\|\mathfrak{e}_{\mathrm{non}}\|_\infty$
Cylinder	$R = 1.0,\ l = 5.0$	406 092	2e+07	0.33	1	24	500 000	500 000	0.026	0.037
Cylinder	$R = 1.0,\ l = 5.0$	406 848	2e+07	0.33	4	4	100 000	1e+06	0.051	0.056
Cube	$a = 5.0,\ b = 5.0,\ c = 5.0$	680 943	2e+07	0.33	1	40	1e+06	1e+06	0.005	0.005
Cube	$a = 5.0,\ b = 5.0,\ c = 5.0$	680 943	2e+07	0.33	4	4	100 000	1.4e+06	0.009	0.009
Plate	$a = 100.0,\ b = 100.0,\ c = 0.7$	680 943	2e+07	0.33	1	34	1.7e+06	1.7e+06	0.064	0.061
Plate	$a = 100.0,\ b = 100.0,\ c = 0.7$	680 943	2e+07	0.33	4	4	100 000	2e+06	0.076	0.062
Beam	$a = 1.0,\ b = 1.0,\ c = 10.0$	521 637	2e+07	0.33	1	6	20 000	20 000	0.019	0.019
Beam	$a = 1.0,\ b = 1.0,\ c = 10.0$	521 637	2e+07	0.33	4	4	1000	30 000	0.028	0.028

z-component of the displacement vector $\boldsymbol{u}$ at the point $(0,0,c)$ is compared between the models, $\mathrm{u}^z{}_{\mathrm{lin}}(0,0,c)$ for the linear model (2) and $\mathrm{u}^z{}_{\mathrm{non}}(0,0,c)$ for the nonlinear model (7). Numerical results are shown in Fig. 3.

3.3. Compression of a cube

The setting is the same as the previous setting of deflection of a thin plate. However, the dimensions a, b and c are now chosen differently—see Table 1 for details—the dimensions are identical hence we talk about a cube instead of a plate. In this case the dimensions of the cube and the Young modulus values are chosen in such a way that they roughly correspond to the values reported in Chandrasekaran et al. (2017); fit of Chandrasekaran et al. (2017, Figure 3; silica aerogel, blue crosses) as reported by Průša et al. (2022).

A part of the top base of the cube is again uniformly loaded, see Fig. 1(d). In particular, the load is uniformly distributed in the square with the side length $\frac{a}{5}$ that located at the centre of the top base. The bottom base is fixed, and the lateral faces are traction free.

The computed quantity x_{diff} is the same as in the case of thin plate deflection, x_{diff} is the relative difference between the deflection of the centre of top base as predicted by the linear model (2) and by the nonlinear model (7). Numerical results are shown in Fig. 4.

3.4. Bending of a beam

We consider a rectangular prismatic beam with the length l and the cross-section dimensions a and b. The left face of the beam is fixed, and a uniformly distributed force $\boldsymbol{F}$ acts at the right beam face. The direction of the force is parallel to this face. (The magnitude of the force $\boldsymbol{F}$ divided by the face area is reported in Table 1 as the load.) The lateral faces are traction free. For overall sketch of the geometry see Fig. 1(e). The values of all relevant parameters are summarised in Table 1.

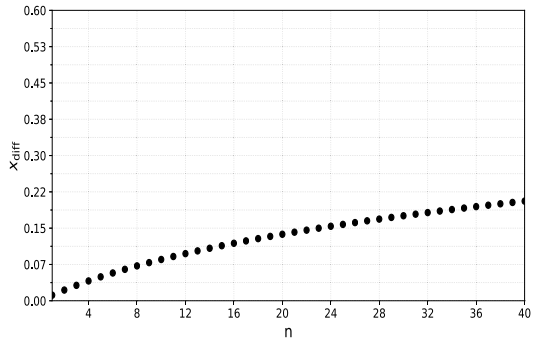

(A) Relative difference between the model predictions x_{diff} as a function of the power-law exponent n; constant applied load.

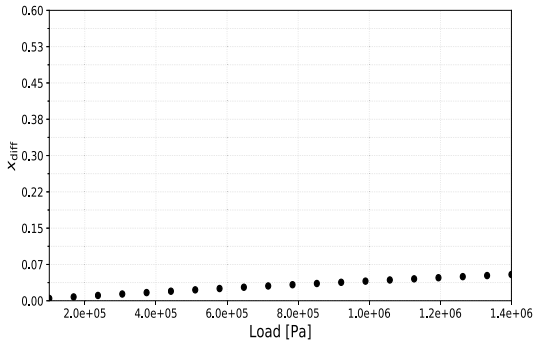

(B) Relative difference between the model predictions x_{diff} as a function of the applied load; constant power-law exponent $n = 4$.

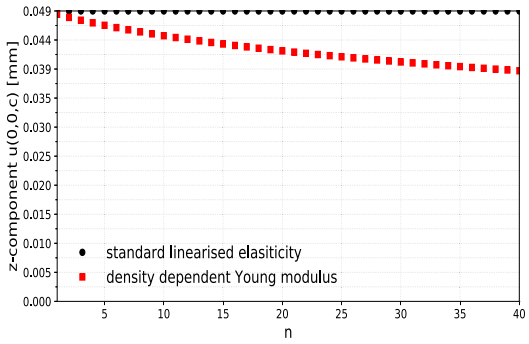

(C) Vertical displacement $\mathrm{u}^z(0,0,0)$ of the top surface centre as a function of the power-law exponent n; constant applied load.

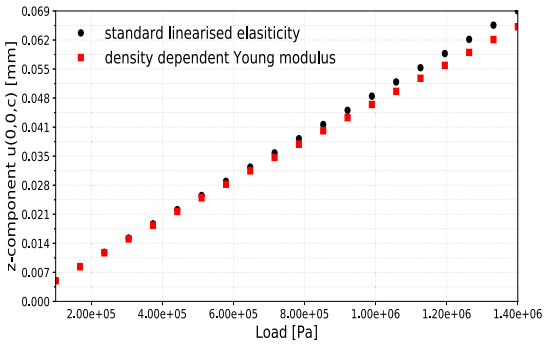

(D) Vertical displacement $\mathrm{u}^z(0,0,0)$ of the top surface centre as as a function of the applied load; constant power-law exponent $n = 4$.

Fig. 4. Compression of a cube, parameters given by Table 1.

The computed quantity x_{diff} is the relative difference between the displacement of the centre of right beam face as predicted by the linear model (2) and by the nonlinear model (7). In other words the absolute value of x-component of the displacement vector at the point $(0, 0, l)$ is compared between the models. Numerical results are shown in Fig. 5.

4. Discussion

The strain values obtained via the solution of corresponding boundary problems always remain in the range commonly accepted as the infinitesimal strain range, see Table 1. The maximum value of linearised strain tensor has been reached in the "plate" setting, but even in this case the pointwise values of linearised strain are bounded by $\|\mathfrak{e}_{\mathrm{non}}\|_\infty = 0.076$. Consequently, we can claim that the infinitesimal strain approximation behind the models is well justified.

The numerical experiments show that the differences between the predictions based on the standard linearised elasticity model (2) and the nonlinear model (7) with the "density dependent Young modulus" can be quite large depending on the value of the power-law exponent n. This is not surprising. However, even for *moderate values of the power-law exponent n that are within the range of values reported in the literature*, see Průša et al. (2022), that is for $n \sim 4$, the difference between the deformation predicted by the standard linearised elasticity model, and the model with the "density dependent Young modulus" *can be still large depending on the particular problem setting*.

If the given boundary problem leads—using the standard linearised model (2)—to the negligible density variations, then the differences between the predictions based on the two models are also negligible, in our case within a few percent. This holds especially for the bending problem, see Section 3.4 and the results shown in Fig. 5. Here, the relative difference between the predictions of both models is less than one percent even for large values of n, see Figs. 5(a) and 5(b).

Larger sensitivity of the results to the choice of the model is observed for the extension of a right circular cylinder and for the compression of a cube, where the differences between the predictions based on both models become evident, see Figs. 2 and 4. In these cases, the relative difference between the predictions can raise up to 20%.

The extreme difference between the predictions based on the two models is observed for the deflection of a thin plate. As one might expect the surface load of a thin plate attached to a fixed foundation leads to substantial density changes directly beneath the loaded part of the surface. Consequently, the deformation prediction based on the model with the "density dependent Young modulus" might be expected to differ substantially from the prediction based on the standard linearised elasticity model. This is indeed the case. The quantity of interest is in this case the relative difference between the z–components of the displacement of the centre of the top (loaded) surface, $x_{\mathrm{diff}} = \frac{|\mathrm{u}^z_{\mathrm{lin}}(0,0,c) - \mathrm{u}^z_{\mathrm{non}}(0,0,c)|}{|\mathrm{u}^z_{\mathrm{lin}}(0,0,c)|}$, and the value of x_{diff} raises up to 50% for $n = 34$, see Fig. 3(a). More importantly, for $n = 4$, which is a realistic value of the power-law exponent, the value of x_{diff} is well above 15%, which is still a substantial difference.

Furthermore, the model with the "density dependent Young modulus" predicts in this case an interesting *qualitative change* in the mechanical response. The standard linearised elasticity model (2) predicts that the deflection of the top surface increases proportionally to the applied load, see Fig. 3(d). However, the model with the "density dependent Young modulus" (7) predicts the deflection to grow slower with the applied load than one might expect based on the standard linearised elasticity model, see Fig. 3. In other words, the material described by the model with the "density dependent Young modulus" behaves, in this case, as if it is getting stiffer with the applied load.

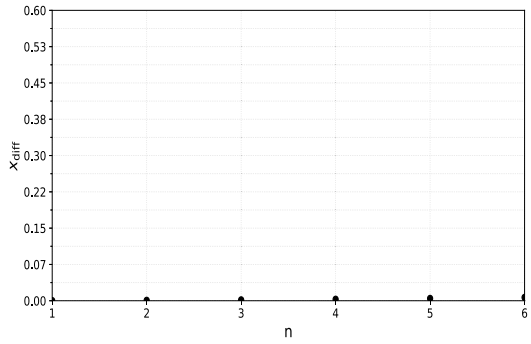

(A) Relative difference between the model predictions x_{diff} as a function of the power-law exponent n; constant applied load.

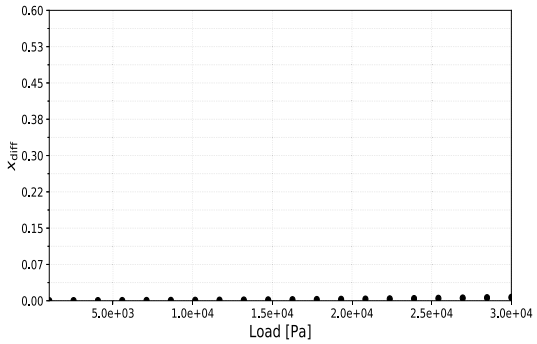

(B) Relative difference between the model predictions x_{diff} as a function of the applied load; constant power-law exponent $n = 4$.

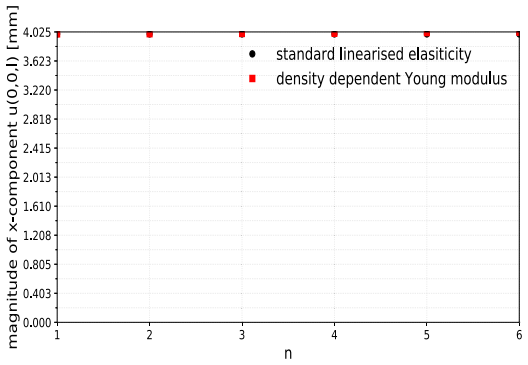

(C) Vertical displacement $\mathrm{u}^x(0,0,0)$ of the right face centre as a function of the power-law exponent n; constant applied load.

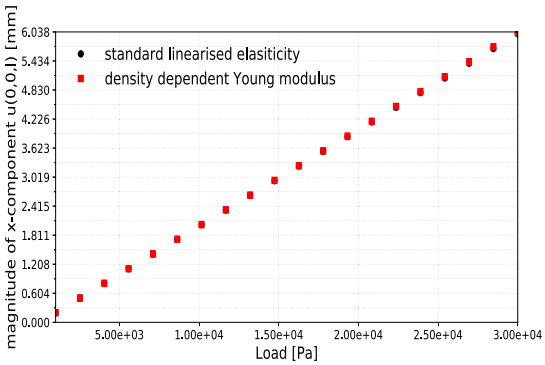

(D) Vertical displacement $\mathrm{u}^x(0,0,0)$ of the right face centre as as a function of the applied load; constant power-law exponent $n = 4$.

Fig. 5. Bending of the beam, parameters given by Table 1.

5. Conclusion

We have investigated the mechanical response of materials described by the standard isotropic linearised elasticity and that of materials with a generalised Young modulus, namely with the "density dependent Young modulus". In particular, we have numerically studied the extension of a right circular cylinder, the deflection of a thin plate, the bending of a beam, and the compression of a cube subject to a surface load, and we have quantified the impact of the "density dependent Young modulus" on the mechanical response in the given setting. In all the cases we have used the infinitesimal strain assumption, and we have *a posteriori* checked that this assumption is satisfied.

In some geometrical settings the impact of the "density dependent Young modulus" is almost nonexisting—the results based on the standard linearised elasticity theory with the constant Young modulus are nearly identical to the results obtained for the density dependent Young modulus. However, in some cases such as the deflection of a thin plate, the results obtained with constant/density dependent Young modulus differ considerably. This observation shows that if the experimental data indicate that there is a need to work with the "density dependent Young modulus", then the mathematical model used for the interpretation of the data must be changed accordingly. The "density dependent Young modulus" should be interpreted as a function of the *current spatially varying density*, which in turn leads to a nonlinear model even under the infinitesimal strain assumption. This applies especially to porous materials such as metal foams, aerogels or bones wherein the concept of "density dependent Young modulus" is frequently used.

Having quantified the difference between the predictions based on the standard linearised elasticity model and the generalised model with "density dependent Young modulus" in the *infinitesimal* strain regime, it would be worthwhile to repeat the same study in the *finite* strain regime. The finite strain models that under the infinitesimal strain assumption lead to the "density dependent Young modulus" have been already proposed, see for example Průša et al. (2020) or Rajagopal and Saccomandi (2022), hence a good starting point for such a study already exists. In the ideal case one should be able to conclude that the infinitesimal strain approximation works as expected—in the infinitesimal strain regime the material response is well captured by the simplified models obtained via the strain linearisation.

Declaration of competing interest

The authors declare the following financial interests/personal relationships which may be considered as potential competing interests: V. P. serves as an Editorial Board Member in the Applications in Engineering Science (the journal which we are submitting).

Data availability

Data will be made available on request.

References

Alnæs, M., Blechta, J., Hake, J., Johansson, A., Kehlet, B., Logg, A., Richardson, C., Ring, J., Rognes, M., Wells, G., 2015. The FEniCS project version 1.5. Arch. Numer. Softw. 3 (100).

Bustamante, R., Rajagopal, K.R., 2020. A review of implicit constitutive theories to describe the response of elastic bodies. In: Merodio, J., Ogden, R. (Eds.), Constitutive Modelling of Solid Continua. Springer, Cham, pp. 187–230.

Bustamante, R., Rajagopal, K.R., 2021. A new type of constitutive equation for nonlinear elastic bodies. Fitting with experimental data for rubber-like materials. Proc. R. Soc. A: Math. Phys. Eng. Sci. 477 (2252), 20210330.

Chandrasekaran, S., Campbell, P., Baumann, T., Worsley, M., 2017. Carbon aerogel evolution: Allotrope, graphene-inspired, and 3D-printed aerogels. J. Mat. Res. 32 (22), 4166–4185.

Gibson, L.J., 2000. Mechanical behavior of metallic foams. Annu. Rev. Mater. Sci. 30 (1), 191–227.

Gibson, I.J., Ashby, M.F., 1982. The mechanics of three-dimensional cellular materials. Proc. R. Soc. Lond. Ser. A Math. Phys. Eng. Sci. 382 (1782), 43–59.

Leventis, N., Sotiriou-Leventis, C., Zhang, G., Rawashdeh, A.-M.M., 2002. Nanoengineering strong silica aerogels. Nano Lett. 2 (9), 957–960.

Logg, A., Wells, G., Mardal, K.-A., 2012. Automated Solution of Differential Equations by the Finite Element Method. Springer Berlin, Heidelberg, p. 731.

Muliana, A., Rajagopal, K.R., Tscharnuter, D., Schrittesser, B., Saccomandi, G., 2018. Determining material properties of natural rubber using fewer material moduli in virtue of a novel constitutive approach for elastic bodies. Rubber Chem. Technol. 91 (2), 375–389.

Murru, P., Rajagopal, K.R., 2021a. Stress concentration due to the bi-axial deformation of a plate of a porous elastic body with a hole. ZAMM–Z. Angew. Math. Mech. 101 (11), e202100103.

Murru, P.T., Rajagopal, K.R., 2021b. Stress concentration due to the presence of a hole within the context of elastic bodies. Mat. Des. Process. Comm. 3 (5), e219.

Průša, V., Rajagopal, K.R., Tůma, K., 2020. Gibbs free energy based representation formula within the context of implicit constitutive relations for elastic solids. Int. J. Non-Linear Mech. 121, 103433.

Průša, V., Rajagopal, K.R., Wineman, A., 2022. Pure bending of an elastic prismatic beam made of a material with density-dependent material parameters. Math. Mech. Solids 28 (8), 1546–1558.

Rajagopal, K.R., 2003. On implicit constitutive theories. Appl. Math. 48 (4), 279–319.

Rajagopal, K.R., 2014. On the nonlinear elastic response of bodies in the small strain range. Acta Mech. 225 (6), 1545–1553.

Rajagopal, K.R., 2018. A note on the linearization of the constitutive relations of non-linear elastic bodies. Mech. Res. Commun. 93, 132–137.

Rajagopal, K.R., 2021. An implicit constitutive relation for describing the small strain response of porous elastic solids whose material moduli are dependent on the density. Math. Mech. Solids 26 (8), 1138–1146.

Rajagopal, K.R., Saccomandi, G., 2022. Implicit nonlinear elastic bodies with density dependent material moduli and its linearization. Int. J. Solids Struct. 234–235, 111255.

Rice, J.C., Cowin, S.C., Bowman, J.A., 1988. On the dependence of the elasticity and strength of cancellous bone on apparent density. J. Biomech. 21 (2), 155–168.

Roberts, A.P., Garboczi, E.J., 2001. Elastic moduli of model random three-dimensional closed-cell cellular solids. Acta Mater. 49 (2), 189–197.

Vajipeyajula, B., Murru, P., Rajagopal, K.R., 2022. Stress concentration due to an elliptic hole in a porous elastic plate. Math. Mech. Solids OnlineFirst.